5' to 3' unfolding directionality of DNA secondary structures by replication protein A: G-quadruplexes and duplexes.

Layal Safa[1,2], Nassima Meriem Gueddouda[3], Frédéric Thiébaut[1,2,4], Emmanuelle Delagoutte[1], Irina Petruseva[5], Olga Lavrik[5], Oscar Mendoza[3], Anne Bourdoncle[3], Patrizia Alberti[1*], Jean-François Riou[1], and Carole Saintomé[1,2*]

[1] Structure et Instabilité des Génomes, Sorbonne Universités, Muséum National d'Histoire Naturelle, INSERM U1154, CNRS UMR 7196, CP26, 57 rue Cuvier, 75005, Paris, France

[2] Sorbonne Universités, UPMC Univ Paris 06, F-75005, Paris, France

[3] Laboratoire ARNA-INSERM U1212, UMR 5320, Institut européen de chimie et biologie, 2 rue Robert Escarpit, 33607 Pessac, France.

[4] Ecole Normale Supérieure - PSL Research University, Département de Chimie, 24 rue Lhomond, CNRS, UMR 7203 LBM, 75005 Paris, France

[5] Novosibirsk Institute of Chemical Biology and Fundamental Medecine, Siberian Division of Russian Academy of Science, 630090 Novosibirsk, Russia.

*To whom correspondence should be addressed. Muséum National d'Histoire Naturelle, INSERM U1154 – CNRS UMR 7196, F-75005, Paris, France, Tel.: (33) 140793686; FAX: (33) 1 40 79 37 05; E-mail: carole.saintome@mnhn.fr ; alberti@mnhn.fr

Running title: RPA unfolds G4s and duplexes with a 5' to 3' directionality

Keywords: Replication Protein A; G-quadruplex; unwinding polarity; G4-ligand; telomeres; gel electrophoresis, fluorescence resonance energy transfer; photocrosslinking; kinetics assay

Abstract

The replication protein A (RPA) is a single-stranded DNA binding protein that plays an essential role in DNA metabolism. RPA is able to unfold G-quadruplex (G4) structures formed by telomeric DNA sequences, a function important for telomere maintenance. To elucidate mechanism through which RPA unfolds telomeric G4s, we studied its interaction with oligonucleotides that adopt a G4 structure extended with a single-stranded tail on either side of the G4. Binding and unfolding was characterized using several biochemical and biophysical approaches and in the presence of specific G4 ligands, such as telomestatin and 360A. Our data show that RPA can bind on each side of the G4 but it unwinds the G4 only from 5' toward 3'. We explain the 5' to 3' unfolding directionality in terms of the 5' to 3' oriented laying-out of hRPA subunits along single-stranded DNA. Furthermore we demonstrate by kinetics experiments that RPA proceeds with the same directionality for duplex unfolding.

Introduction

Human telomeres are composed of tandem repeats of the sequence 5'-TTAGGG-3' and bear a 3' single-stranded extension (also known as 3' G-overhang). This G-rich telomeric single-stranded extension can adopt non-canonical DNA conformations known as G-quadruplexes (G4s) (1). These four-stranded structures are based on guanine quartets stabilized by Hoogsteen hydrogen bonds; these structures are stabilized by cations in the central cavity. The human telomeric sequence can form intramolecular G4 of different conformations (2). There is evidence that G4 forms in cells at telomeres during lagging strand DNA replication and at the 3' G-overhang (3-6). Several proteins interact with telomeric G4s to regulate telomerase activity and

maintain telomere integrity (7). Among them, the replication protein A (RPA) has been shown to have a key role in telomere maintenance and telomerase action (8-14).

RPA is a highly conserved protein in eukaryotes (15, 16); it is involved in essential processes such as replication, recombination, and DNA repair (17). RPA is a heterotrimeric protein composed of RPA1, RPA2, and RPA3 subunits. RPA carries six DNA-binding domains (DBD), four of them are located in RPA1 (DBD-A, DBD-B, DBD-C and DBD-F), one is located in RPA2 (DBD-D), and one in RPA3 (DBD-E). RPA binds to unstructured, single-stranded DNA (ssDNA) through three different binding modes involving five of the six DBD domains: DBDs A, B, C, D, and E (17-19). It is now accepted that RPA binds to ssDNA in a sequential pathway with a defined polarity (20, 21). First, the high-affinity DBD-A and DBD-B domains of RPA1 bind to 8-10 nucleotides (nt) (22); this initial binding is designated as the "compact" conformation or 8-10-nt binding mode. This step is followed by weaker interactions of DBD-C of RPA1 with the 3' side of the ssDNA, leading to an intermediate named "elongated contracted" conformation or 13-22-nt binding mode (18, 23, 24). Finally, binding of DBD-D of RPA2 and DBD-E of RPA3 to the 3' side of the ssDNA leads to a stable "elongated extended" complex in which RPA covers 30 nt (30-nt binding mode); this is the most stable RPA/ssDNA complex (18). RPA binds ssDNA in a non-sequence specific manner (15); however it has a higher affinity for pyrimidine sequences than for other sequence compositions. Recently, Prakash et al. showed, using a SELEX experiment, that DBD-A and DBD-B preferentially bind pyrimidine-rich sequences, DBD-C has no sequence preference, and DBD-D and DBD-E bind G-rich sequences (25).

In 2006, RPA was shown to unfold telomeric G4 structures *in vitro* (26). Since

2

then, many studies have focused on the interaction between RPA and G4 in order to determine its unfolding mechanism. Electrophoretic mobility shift assays (EMSA) and fluorescence resonance energy transfer (FRET) experiments indicate that the initial binding of the human RPA (hRPA) requires a ssDNA region (27), probably generated by G4 structural breathing that transiently exposes ssDNA (28-30), and that this initial step is rate limiting (31, 32). Second, an inverse relationship between telomeric G4 structural stability and hRPA binding has been established (27, 33). Third, the hRPA binding mode (1:1 complexes where one RPA is bound on the DNA in an elongated mode, or 2:1 complexes where two RPA are bound on the DNA in a compact mode) depends on hRPA concentration (18, 27). Fourth, crosslinking experiments showed that the RPA1 and RPA2 subunits of the hRPA directly contact the G4 sequence (27). These data were recently confirmed by the characterization of the RPA1-D228Y mutation that impaired both the binding and the opening of the telomeric G4 (34). In addition, it has been shown that hRPA binds G4 DNA in a 5' to 3' spatial manner (27) in agreement with its polarity of binding to unstructured ssDNA (18, 21, 35) and to a non-telomeric G4 (25). Based on these data, we have suggested a sequential hRPA-mediated G4 unfolding mechanism where hRPA unfolds G4 with a 5' to 3' directionality, however experimental evidence of such a directionality is still missing (27). Here, we have performed a set of experiments combining the use of a telomeric G4 sequence extended by a ss-tail on either side of the G4 sequence and the use of G4-ligands, to provide experimental evidence that hRPA unfolds G4 according to a 5' to 3' directionality and to unravel the reasons of this directionality.

Results

EMSA experiments show that the presence of a single-stranded tail attached to the telomeric G4 enhances hRPA binding - We investigated, by electrophoretic mobility shift assay (EMSA), how a single-stranded tail attached to either end of the htelo G4 sequence impacted the efficiency of binding of the G4 structure by hRPA. We designed four modified versions of the htelo G4 (Table 1): 1) 5t-htelo with a single-stranded tail of five thymidines on the 5' side of the G4, 2) htelo-5t with a single-stranded tail of five thymidines on the 3' end, 3) 10t-htelo with a single-stranded tail of 10 thymidines on the 5' end, and 4) htelo-10t with a single-stranded tail of 10 thymidines on the 3' side. The CD spectra of these extended htelo sequences did not strongly differ from the spectrum of the original htelo (data not shown), suggesting that the single-stranded tails did not affect the G4 conformation. The presence of a single-stranded tail decreased the melting temperature (Tm) of the G4 structure (Table 1). Compared to the htelo oligonucleotide, a single-stranded tail at the 5' end decreased the Tm by about 9 °C and a single-stranded tail at the 3' end decreased the Tm by about 7 °C; the extent of destabilization was nearly independent of the length of the tail.

hRPA binding to these extended htelo sequences was studied by EMSA on a native agarose gel (Figure 1A). Slow migrating species corresponding to hRPA:DNA complexes appeared for htelo and extended htelo DNAs as the protein concentration increased. Quantification of the EMSA clearly revealed that the presence of a single-stranded tail increased the affinity of hRPA for the G4 oligonucleotide (Figures 1B and C) and that hRPA affinity was proportional to the length of the tail. Indeed, the concentration of hRPA required to complex 50% of the DNA was 60 nM for htelo, 25 nM for 5t-htelo and htelo-5t, and 18 nM for 10t-htelo and htelo-10t. This indicates that a single-

3

stranded region of 5 or 10 nt on either side of the G4 formed by htelo enhances binding of hRPA.

FRET experiments show that hRPA efficiently unfolds the telomeric G4 structures with single-stranded tails - To determine whether binding of hRPA to the extended 10t-htelo and htelo-10t oligonucleotides resulted in unfolding of the G4 structure, we carried out fluorescence resonance energy transfer (FRET) experiments with these extended oligonucleotides labeled with a FAM and a TAMRA at the 5' and 3' end of the G4 region, respectively (Table 1). Melting experiment showed that both extended labeled G4s have the same stability (curves not shown, *Tm* reported in Table 1). Fluorimetric titrations of 10t-FhteloT and FhteloT-10t with hRPA were performed, and data were quantified to determine the energy transfer efficiency (P, defined in Experimental procedures section) as a function of hRPA/DNA ratio (r). With both oligonucleotides, the P value increased as the ratio r increased (Figure 1D) indicating that FRET was suppressed by the addition of protein to DNA. The maximal P value was nearly the same as the one previously obtained for the non-extended FhteloT (27). These results demonstrate that hRPA completely unfolds the G4 structure of the extended htelo oligonucleotides, irrespective of whether the single-stranded region is at 5' or 3' side of the G4.

Crosslinking experiments show that hRPA binds the extended G4 structures via its RPA1 and RPA2 subunits - To determine the positioning of hRPA along the extended telomeric G4 sequence, a photo-crosslinking strategy based on thionucleobases was applied (18, 36-38). Eight different extended oligonucleotide analogues containing a single photoactivable 4-thiothymine residue (s^4T), at the extremity of the single-stranded extension, at the 5' side of the G4, in the middle of the G4 and at the 3' side of the G4, were used (Table 1). Upon UV

irradiation of the hRPA-DNA complex, the s^4T residue can form a covalent bond linking the DNA with the protein.

Photo-crosslinked complexes obtained in the presence of 20 nM hRPA and 2 nM htelo-S DNA were resolved by SDS-PAGE. At these concentrations, the major stoichiometry of the hRPA:htelo complex was 1:1 (26, 27). No crosslinks were formed without UV-irradiation (data not shown). Upon UV-irradiation, in addition to the free radioactively labeled DNA band, two bands of radioactively labeled products with low electrophoretic mobility appeared (Figure 2). The apparent molecular weights of the species present in these bands were 35 kDa and 90 kDa, consistent with DNA crosslinking to the RPA2 and RPA1 subunits, respectively (27). Despite the length of extended htelo is sufficient to allow RPA3 interacting with the DNA (18), we did not detect any crosslink between this subunit and the extended htelo. We conclude from these crosslinking experiments that hRPA interacts with the extended htelo sequences via its RPA1 and RPA2 subunits.

To establish the relative position of each subunit on DNA, we calculated the relative percentage of the crosslinked species. We observed that RPA1 was primarily crosslinked on the 5' side of the DNA, whereas RPA2 was located on the 3' side (Figure 2). Thus, these results are in agreement with a 1:1 stoichiometry and show that hRPA binds extended htelo G4 with a 5' to 3' polarity (i.e., RPA1 and RPA2 are bound at the 5' and 3' sides of the oligonucleotides, respectively). This result is in accordance with results we previously obtained with the 21-nt telomeric G4 (htelo) (27) and with a 31-nt oligo-dT (26). In addition, crosslinking experiments also showed that in the 1:1 complexes, hRPA covered the entire length of the unfolded 10t-htelo and htelo-10t oligonucleotides, indicative of the 'elongated extended' complex, which is a 30-nt binding mode.

4

The presence of G4 ligands reveals a decreased binding affinity of hRPA for 5' extended htelo and suggests a 5' to 3' directionality of the G4 unfolding - EMSA and FRET did not reveal any hRPA unfolding directionality. We decided to investigate the effect of G4 stabilizing ligands (39) on binding and unfolding by hRPA. Indeed, a stabilizing G4 ligand strongly diminishes the unfolded or partially folded intermediate states, constraining RPA to mainly interact with the single-stranded tails located at the 5' and 3' side of the G4 formed by extended htelo. We used telomestatin and the pyridine dicarboxamide derivatives 360A and 360A-Br (structures shown in (27)), that are remarkably selective for G4 relative to duplex DNA (40-42).

Melting experiments followed by FRET indicated that each of the three ligands stabilized to a similar extent both the extended G4 structures 10t-FhteloT and FhteloT-10t, independently of the orientation of the extension (ΔTm = 20 °C for 1 mM 360A and 360A-Br; ΔTm = 20 °C for 1 mM telomestatin, in KCl 10 mM plus LiCl 90 mM). Interestingly, in EMSA experiments, the presence of telomestatin decreased the affinity of hRPA for all four extended htelo sequences, but to different extents (Figures 3A and 3B). Binding of hRPA to htelo bearing 5-nt tails was strongly impaired (around 60% of inhibition) whether the tails was on the 5' or 3' side of the G4 (Figure 3A). This result suggests that when the G4 structure is strongly stabilized by a G4 ligand, a single-stranded tail of 5 nt is not sufficient to allow binding of hRPA. The presence of 10-nt single-stranded tails allowed hRPA to bind to the oligonucleotides in the presence of telomestatin (Figure 3B). Importantly, the affinity of hRPA depended on the position of the tail: hRPA bound 10t-htelo les efficiently than htelo-10t. This behavior was observed not only with telomestatin but also with 360A and a 360A-Br (Figure 3C), showing that the difference in the binding between htelo-10t

and 10t-htelo was not due to the nature of the ligand. These results show that hRPA has a lower binding efficiency to single-stranded regions at the 5' side of the G4 structure than to single-stranded tails at the 3' side as previously observed on hairpin and duplex structures (43, 44).

To investigate whether binding of hRPA to 10t-htelo and htelo-10t in the presence of G4 ligand results in G4 unfolding, we carried out FRET experiments in the presence of 360A with both 10t-FhteloT and FhteloT-10t DNAs (Figure 3D). Results show that hRPA open the G4 when the ss extension is at its 5' side (the P value increased from 0.3 to 0.8), while the G4 bearing the ss tail at its 3' side was poorly opened (the P value increased from 0.35 to 0.5). We point out that, in the absence of hRPA (r = 0), the P value in the presence of ligand was higher than in the absence of ligand (0.35 vs 0.15). This is due to the fact that 360A quenches TAMRA emission to a larger extent than FAM emission, as verified with htelo labeled with a single FAM at the 5' terminus or with a single TAMRA at 3' end showed that 360A (data not shown). Quenching of FRET processes by G4 ligands is a well-known phenomenon (45). Hence, on one hand EMSA experiments in the presence of 360A show that hRPA binds to both 10t-htelo and htelo-10t, with a higher affinity for structures bearing a protruding 3' tail; on the other hand FRET experiments show that hRPA unwinds the G4 structure only when the single-stranded tail is on the 5' side of the G4, suggesting a 5' to 3' directionality in G4 unfolding by hRPA.

To ascertain that the observed 5' to 3' directionality in G4 unfolding was not due to the nature of the two fluorophores (i.e. to a different effect of FAM and TAMRA on the interaction of hRPA with the extended oligonucleotides), we initially designed the inverted systems bearing a TAMRA at the 5' side and a FAM at the 3' side of the G4. Unluckily 10t-ThteloF was less stable than ThteloF-10t, as revealed by

5

FRET, making the inverted systems not suitable for such control experiment (data not shown).

Kinetic experiments reveal a 5' to 3' of unfolding directionality by hRPA - To further investigate the directionality of DNA unfolding by hRPA, we conceived a kinetic experiment based on a recently published helicase assay (46). We used four different DNA constructs (sequences are listed in Table 2). The first construct (11ss-htelo-dx) is the one used by Mendoza et al.; it is composed of a 11 nt single-stranded tail at the 5' side of the htelo sequence and of a 15 bp duplex region (at the 3' side of the G4) labeled with a FAM and a Dabcyl dye allowing detecting the unwinding of the construct by fluorescence emission (Figure 4A, inset). Two nucleotides separate the G4 from the duplex structure; this short spacer is not expected to provide a binding site for hRPA (23). Here we designed a symmetrical construct (dx-htelo-11ss) bearing the single-stranded tail at the 3' end (Figure 4B, inset). The two symmetrical DNA constructs had similar melting profiles (not shown), making them suitable for the study of unfolding by hRPA. Finally we tested two additional constructs where the htelo sequence was replaced by a non-G4 sequence (named "mut") not able to fold into a G4 (Figures 4C and 4D, insets). Results showed that hRPA opened the constructs with the protruding 5' single-strand, but not the constructs with the 3' protruding single-strand (Figure 4). A better efficiency to open duplex with a 5' single-stranded tail has already been reported (43, 47). The opening curves of 11ss-htelo-dx were identical to the opening curves of 11ss-mut-dx, indicating that the opening of the duplex was the rate-limiting step of the unfolding of the construct.

Although this assay does not allow directly monitoring G4 unfolding but the final disruption of the duplex, it shows that unwinding by hRPA of the construct containing a G4 proceeds in the 5' to 3' direction, in agreement with our FRET experiments. In addition, we confirm that hRPA is able to open duplex structures (43, 47-49), and soundly demonstrate, for the first time, by kinetics experiments, that duplex unwinding proceeds in the 5' to 3' direction.

Discussion

In this work, we investigated the mechanism of G4s unfolding by hRPA. To this purpose, we studied the interaction of hRPA with oligonucleotides that adopt a G4 structure extended with a single-stranded tail on either side of the G4, in the absence or in the presence of a G4 stabilizing ligand.

We first showed that a single-stranded region of 5 or 10 nt on either side of the G4 enhanced binding of hRPA. This can be explained by two factors. On one hand, the G4s formed by the extended htelo have a lower stability than the G4 formed by htelo, and, as we previously showed, a decrease in G4 stability increases the binding affinity of hRPA (26,27). On the other hand, the presence of single-stranded tails increases the number of potential hRPA binding sites (15, 16). Interestingly, Pif1 helicase was also reported to bind more efficiently to a single-stranded-tailed G4 than a tailless G4 (50).

On one side, EMSA and FRET showed that, in the absence of G4 stabilizing ligands, hRPA bound and unfolded the G4 structure formed by the extended htelo oligonucleotides, regardless of whether the single-stranded extension was at the 5' or the 3' side. On the other side, EMSA and FRET in the presence of G4 stabilizing ligands revealed a surprising behavior: hRPA bound to both extended htelo oligonucleotides, however it efficiently unwound only the G4 bearing a single-stranded extension at its 5' side, suggesting that hRPA unfolds G4s from 5' toward 3'. Moreover, a kinetic assay allowed

6

unambiguously demonstrating a 5' to 3' unfolding directionality on duplex structures. Hence, overall, our results support that hRPA unfolds G4s and duplexes according to a 5' to 3' directionality.

Interestingly, hRPA 5' to 3' unfolding directionality is in agreement with results we obtained in a recent study of a mutation in RPA1 (D228Y), which alters the ability of hRPA to bind DNA and in particular G4 sequences and causes dramatic telomeric replication defects in fission yeast (Rpa1-D223Y strain) (34). We showed that over-expression of the 5' to 3' Pif1 helicase family members (51, 52) rescues the telomere defects of the Rpa1-D223Y strain, whereas over-expression of the 3' to 5' helicase Rqh1 (53) or Pot1 that unfolds G4 from 3' to 5' (54) did not.

This 5' to 3' unfolding directionality can be explained in terms of the 5' to 3' oriented laying-out of hRPA subunits along single-stranded DNA (Figure 5A). The spatial polarity, previously observed for ss DNA and for the htelo sequence, has been here confirmed for extended G4 by crosslinking experiments. When hRPA binds next to the 5' side of a G4, its laying-out toward 3' destabilizes and unfolds the G4 structure "in front" of it (Figure 5B). Conversely, when it binds next to the 3' side of a G4, its laying-out toward 3' does not affect the G4 structure (Figure 5C) "behind" it.

In the absence of ligands, hRPA can interact with the single-stranded tails located at the 5' and 3' side of the G4, but also with transiently accessible single-stranded regions of the G4 core sequence (28-30). Whereas, in the presence of stabilizing ligands, hRPA is constrained to mainly interact with the single-stranded tails. For this reason, the unfolding directionality was revealed only by experiments with extended htelo sequences in the presence of G4 stabilizing ligands.

EMSA in the presence of a ligand also revealed a decrease in hRPA binding efficiency to the htelo with a 5' extension. This might be explained by the 5' to 3' binding directionality of hRPA with respect to the single-stranded DNA. When hRPA binds to a few nucleotides next to the 5' side of a highly stable G4 in the 8-10 nt binding mode, the DBD-C of RPA1 and DBD-D of RPA2 are oriented toward 3' (21), where the G4 is located; the G4 may hence physically hinder the interaction of hRPA with the DNA. A lower binding efficiency of hRPA to a 5' protruding single-stranded tail has already been reported for a hairpin and duplex structures with 5' or 3' single-stranded tails of 10-19 nt (43, 44).

In conclusion, our work demonstrates that hRPA unfolds G4s and duplexes from 5' to 3'. Interestingly our results (present and previous) show that hRPA opens more easily the htelo G4 than the duplex. Indeed 20 equivalent of hRPA were needed to obtain a fraction of unfolded duplex (ss-mut-dx) of about 0.7 and equilibrium was attained in about 30 min (Figure 4); while only 5 equivalent of hRPA were needed to obtain the same unfolded fraction of htelo G4 and equilibrium was attained in less than 30 s (see Figure 7 in 26). Likely, the unwinding mechanisms of G4s and duplexes are different. On one hand, the relative fast kinetics and the stoichiometric conditions of G4 unfolding supports that the unfolding directionality of G4s results from the sequential binding of the subunits of a single hRPA to DNA from 5' toward 3'. On the other hand, the relative slow kinetics and the high amount of hRPA needed to unfold the duplex suggests that duplex unfolding might result from a cooperative binding of hRPA proteins in the compact 8-10 nt binding mode (23).

Thus, even if hRPA is not a helicase, it is able to unfold G4s, in addition to duplexes, with the same defined 5' to 3' unwinding polarity. In contrast to helicases that require ATP hydrolysis to

unwind nucleic acid duplexes in a polar manner (55-57), hRPA does it in an energy-independent manner. It is possible that the polar unwinding activity of hRPA stems from its sequential binding mode involving intermediates with increasing binding site sizes. In addition, the polar unwinding activity of hRPA that we report in this study may facilitate the oriented access of specific proteins on single-stranded DNA. In particular, the ability of hRPA to unfold G4s from 5' to 3' is consistent with its important role in unfolding G4 structures on the lagging strand during telomere replication (Figure 5D) (34).

Experimental procedures

Materials - BSA was from Roche, $\gamma[^{32}P]ATP$ was from PerkinElmer, and T4 polynucleotide kinase (PNK) was from NEW England BioLabs. Oligonucleotides were purchased from Eurogentec (Belgium). The sequences of the oligonucleotides used are listed in Tables 1 and 2. DNA concentrations were determined by UV spectroscopy using the extinction coefficients provided by the manufacturer. Recombinant hRPA was expressed in the *Escherichia coli* BL21 (DE3) strain transformed with the plasmid pET$_{11a}$-hRPA that permits the co-expression of RPA1, RPA2, and RPA3. hRPA was purified using Affi-Gel Blue, hydroxyapatite (Biorad), and Q-Sepharose chromatography columns as previously described (58). Telomestatin was a generous gift from Kazuo Shin-ya (University of Tokyo, Japan). The pyridine dicarboxamide derivatives 360A and 360A-Br were synthesized by Patrick Mailliet in our laboratory and by Marie-Paule Teulade-Fichou (Institut Curie, Orsay, France), respectively. Telomestatin, 360A, and 360A-Br were dissolved at 10 mM in DMSO immediately before use.

Electrophoretic mobility shift assay - Oligonucleotides were labeled with $\gamma[^{32}P]ATP$ using T4 polynucleotide kinase. Non-incorporated $\gamma[^{32}P]ATP$ was removed using a Biospin 6 column (Bio-Rad) equilibrated in TE buffer. For all EMSA experiments, hRPA was diluted and pre-incubated (10 min at 4 °C) in buffer containing 50 mM Tris-HCl (pH 7.5), 100 mM KCl, 1 mM DTT, 10% glycerol, 0.2 mg/mL BSA, and 0.1 mM EDTA. In a standard reaction, radiolabeled oligonucleotide (2 nM) was incubated with various amounts of protein in 10 µL reaction buffer [50 mM HEPES (pH 7.9), 0.1 mg/ml BSA, 100 mM KCl, and 2% glycerol] for 15 min at 20 °C. Longer incubation times (up to 1 h) did not affect the patterns or intensities of the bands, indicating that the system had reached thermodynamic equilibrium within 15 min. Samples were then loaded on a native 1% agarose gels in 0.5X TBE buffer. Electrophoresis was performed for 90 min at 5 V/cm at room temperature. After electrophoresis, the gel was dried and exposed to a phosphorimager screen. After being exposed for at least 10 h, the screen was scanned with the Phosphorimager TYPHOON instrument (Molecular Dynamics). The band intensities were quantified using ImageQuant version 5.1. For each hRPA concentration, the fraction of radiolabeled oligonucleotide bound to hRPA was calculated as follow: $I_{DNA\ bound\ to\ hRPA} / (I_{free\ DNA} + I_{DNA\ bound\ to\ hRPA})$. Each experiment was reproduced at least twice. When indicated, error bars correspond to the standard deviation calculated from at least two independent experiments. When G4 ligands were used, radiolabeled oligonucleotide (2 nM) was pre-incubated with 0.5 µM G4 ligand for 10 min at room temperature in the standard reaction buffer before adding hRPA.

Thermal melting studies - UV-melting profiles were acquired on an Uvikon XL spectrometer (Secoman). The oligonucleotide were dissolved in 50 mM

HEPES (pH 7.9) and 100 mM KCl, at 3 μM strand concentration. Samples were heated at 90 °C for a few minutes, cooled to 5 °C, kept at 5 °C for 30 min, heated to 90 °C, and cooled to 5 °C; heating and cooling were done at 0.2 °C/min. Absorbance of oligonucleotides was recorded at 245, 260, 273, 295, and 400 nm as a function of temperature. Melting temperatures (Tm) were defined as the intercept between the melting curve at 295 nm and the median line between low-temperature and high-temperature absorbance linear baselines. At the end of melting experiences, CD spectra were collected, at 5 °C, on a J-810 spectropolarimeter (Jasco). Fluorescence melting profiles of oligonucleotides labeled with 6-carboxyfluoresceine (FAM) and tetramethylrodamine (TAMRA) were recorded on a MX3000P (Stratagene) at a strand concentration of 0.2 μM in 10 mM cacodylic acid (pH 7.2) supplemented with 10 mM KCl and 90 mM LiCl, or with 100 mM KCl. The temperature was increased from 25 to 95 °C at 1 °C/min and the emission was recorded as a function of temperature (excitation wavelength 492 nm and emission wavelength 516 nm). Fluorescence melting profiles were normalized between the maximum and the minimum of fluorescence and Tm was defined as the temperature at which the normalized fluorescence intensity was equal to 0.5.

Fluorescence titrations assay - Fluorescence spectra of 100 nM 10t-FhteloT or FhteloT-10t oligonucleotides were recorded at 20 °C in a buffer containing 50 mM KCl, 2 mM MgCl$_2$, and 5 mM lithium cacodylate (pH 7.2). 10t-FhteloT or FhteloT-10t was pre-incubated (10 min at 20 °C) with or without 0.5 μM G4 ligand. The protein (from 100 to 1000 nM) was directly added to the solutions containing the oligonucleotides alone or in the presence of the G4 ligand. The spectra (490 to 660 nm) were collected after 2 min of incubation while exciting at 470 nm.

The fluorescence intensity of fluorophore was measured at 518 nm (I_D) for the donor FAM and at 586 nm (I_A) for the acceptor TAMRA. The ratio P was calculated as $P = I_D/(I_D + I_A)$, where I_D and I_A are the emission intensities of the donor FAM and of the acceptor TAMRA, respectively.

Fluorescence kinetic assay – All oligonucleotides used in this assay are listed in Table 2. DNA constructs (11ss-htelo-dx and dx-htelo-11ss, 11ss-mut-dx and dx-mut-11ss) were prepared by annealing a mixture of Dabcyl-labeled oligonucleotide (1μM) and FAM-labeled oligonucleotide (0.85μM), in 20 mM Tris-HCl buffer (pH 7.3) containing 5 mM MgCl$_2$, 1mM KCl and 99 mM NaCl. Mixtures were heated 5 min at 90 °C and then slowly cooled to room temperature. DNA samples were then stored at -20 °C. Unfolding reactions were carried out at least in triplicate in 96-well plates at 25 °C and fluorescence monitored in a microplate reader Infinite M1000 PRO (Tecan). Every replicate, containing 50μl solution of 10 nM of DNA construct (previously prepared at 1μM) and 100 nM of an oligonucleotide complementary to the FAM-labeled strand (named Trap1 in Table 2), was incubated with the indicated amount of hRPA (0, 10, 20, 50, 100, 150 or 200 nM). The 96-well plate was stirred for 10 s and the fluorescence emission recorded every 10 s. The excitation wavelength was set at 492 nm and the emission wavelength at 520 nm. Once the steady-state was attained (after about 30–45 min), 100 nM of an oligonucleotide complementary to the Dabcyl-labeled sequence (named Trap2 in Table 2) was added to reaction wells in order to completely unfold the DNA construct. Well-plates were then stirred for 10 s, and emission monitored every 10 s until reaching again the steady-state of fluorescence emission. For each DNA construct, the fluorescence emission as a function of time was then normalized between the minimal and maximal values. In order to check the stability of 11ss-htelo-dx and dx-htelo-11ss DNA

9

constructs, UV melting experiments were carried out with an UVmc2 spectrophotometer (SAFAS). Samples were heated at 96.5 °C for five minutes, then cooled from 96.5 °C to 0.5 °C, kept at 0.5 °C for ten minutes, and then heated from 0.5 to 96.5 °C with a rate of 0.2 °C /min. The absorbance as a function of temperature was monitored at 335, 295, 273, 260 and 240 nm.

Photo-crosslinking experiments - Radiolabeled oligonucleotides (2 nM) were mixed with the indicated amount of protein using the protocol described in the EMSA section. Each sample (20 μL) was irradiated for 30 min at 10 °C at 360 nm. Laemmli gels (10%) were used to separate crosslinked species.

Conflict of interest: The authors declare that they have no conflicts of interest with the contents of this article.

Author contributions: CS and JFR designed the study; CS, JFR and PA wrote the manuscript; LS performed EMSA, fluorescence titration and crosslinking assays; LS, FT, IP, and ED prepared hRPA; PA carried out UV and FRET melting experiments and collected CD spectra; NG performed fluorescence kinetic assays; NG, AB and OM analyzed kinetic assays; OL contributed to the discussion of data; All authors revised and approved the final version of the manuscript.

10

REFERENCES

1. Davis, J.T., Spada, G.P. (2007) Supramolecular architectures generated by self-assembly of guanosine derivatives. *Chem. Soc. Rev.* **36**, 296-313

2. Phan, A.T. (2010) Human telomeric G-quadruplex: structures of DNA and RNA sequences. *Febs J.* **277**, 1107-1117

3. De Cian, A., Lacroix, L., Douarre, C., Temime-Smaali, N., Trentesaux, C., Riou, J.F., Mergny, J.L. (2008) Targeting telomeres and telomerase, *Biochimie* **90**, 131-155

4. Lipps, H.J., Rhodes, D. (2009) G-quadruplex structures: in vivo evidence and function. *Trends Cell Biol.* **19**, 414-422

5. Biffi, G., Tannahill, D., Mc Cafferty, J., Balasubramanian, S. (2013) Quantitative visualization of DNA G-quadruplex structures in human cells. *Nat. Chem.* **5**, 182-186

6. Henderson, A., Wu, Y., Huang, Y.C., Chavez, E. A., Platt, J., Johnson, F.B., Brosh, R.M., Sen, D., Lansdrop, P.M. (2014) Detection of G-quadruplex DNA in mammalian cells. *Nucleic Acids Res.* **42**, 860-869

7. Brázda, V., Hároníková, L., Liao, J.C., Fojta, M. (2014) DNA and RNA quadruplex-binding proteins. *Int J Mol Sci.* **15**, 17493-17517

8. Smith, J., Zou, H., Rothstein, R. (2000) Characterization of genetic interactions with RFA1: the role of RPA in DNA replication and telomere maintenance. *Biochimie* **82**, 71-78

9. Kibe, T., Ono, Y., Sato, K., Ueno, M. (2007) Fission yeast Taz1 and RPA are synergistically required to prevent rapid telomere loss. *Mol. Biol. Cell.* **18**, 2378-2387

10. Kobayashi, Y., Sato, K., Kibe, T., Seimiya, H., Nakamura, A., Yukawa, M., Tsuchiya, E., Ueno, M. (2010) Expression of mutant RPA in human cancer cells causes telomere shortening. *Biosci. Biotechnol. Biochem.* **74**, 382-385

11. Luciano, P., Coulon, S., Faure, V., Corda, Y., Bos, J., Brill, S.J., Gilson, E., Simon, M.N., Geli, V. (2012) RPA facilitates telomerase activity at chromosome ends in budding and fission yeasts. *EMBO J.* **31**, 2034-2046

12. Schramke, V., Luciano, P., Brevet, V., Guillot, S., Corda, Y., Longhese, M.P., Gilson, E., Geli, V. (2004) RPA regulates telomerase action by providing Est1p access to chromosome ends. *Nat. Genet.* **36**, 46-54

13. Grudic, A., Jul-Larsen, A., Haring, S.J., Wold, M.S., Lonning, P.E., Bjerkvig, R., Boe, S.O. (2007) Replication protein A prevents accumulation of single-stranded telomeric DNA in cells that use alternative lengthening of telomeres. *Nucleic Acids Res.* **35**, 7267-7278

14. Cohen, S., Jacob, E., Manor, H. (2004) Effects of single-stranded DNA binding proteins on primer extension by telomerase. *Biochim. Biophys. Acta* **1679**, 129-140

15. Wold, M.S. (1997) Replication protein A: a heterotrimeric, single-stranded DNA-binding protein required for eukaryotic DNA metabolism. *Annu. Rev. Biochem.* **66**, 61-92

16. Iftode, C., Daniely, Y. and Borowiec, J.A. (1999) Replication protein A (RPA): the eukaryotic SSB. *Crit Rev Biochem. Mol. Biol.*, **34**, 141-180

17. Oakley, G.G. and Patrick, S.M. (2012) Replication protein A: directing traffic at the intersection of replication and repair. *Front. Biosci.* **15**, 883-900

18. Romero Salas, T.R., Petruseva, I., Lavrik, O. and Saintome, C. (2009) Evidence for direct contact between the RPA3 subunit of the human replication protein A and single-stranded DNA. *Nucleic Acids Res.* **37**, 38-46

19. Cai, L., Roginskaya, M., Qu, Y., Yang, Z., Xu, Y. and Zou, Y. (2007) Structural characterization of human RPA sequential binding to single-stranded DNA using ssDNA as a molecular ruler. *Biochemistry* **46**, 8226–8233

20. Bochkareva, E., Korolev, S., Lees-Miller, S.P. and Bochkarev, A. (2002) Structure of the RPA trimerization core and its role in the multistep DNA-binding mechanism of RPA. *EMBO J.* **21**, 1855–1863

11

21. Kolpashchikov, D.M., Khodyreva, S.N., Khlimankov, D.Y., Wold, M.S., Favre, A. and Lavrik,O.I. (2001) Polarity of human replication protein A binding to DNA. *Nucleic Acids Res.* **29**, 373–379

22. Bochkarev, A., Pfuetzner, R.A., Edwards, A.M. and Frappier, L. (1997) Crystal structure of the DNA binding domain of replication protein A bound to DNA. *Nature* **385**, 176–181

23. Lavrik, O.I., Kolpashchikov, D.M., Weisshart, K., Nasheuer, H.P., Khodyreva, S.N. and Favre, A. (1999) RPA subunit arrangement near the 3'-end of the primer is modulated by the length of the template strand and cooperative protein interactions. *Nucleic Acids Res.* **27**, 4235–4240

24. Bochkareva, E., Belegu, V., Korolev, S. and Bochkarev, A. (2001) Structure of the major single-stranded DNA-binding domain of replication protein A suggests a dynamic mechanism for DNA binding. *EMBO J.* **20**, 612–618

25. Prakash, A., Natarajan, A., Marky, L.A., Ouellette, M.M., Borgstahl, G.E (2011) Identification of the DNA-binding domains of human replication protein a that recognize G-quadruplex DNA, *J. Nucleic Acids*, 896947

26. Romero Salas, T.R., Petruseva, I., Lavrik, O., Bourdoncle, A., Mergny, J.L., Favre, A., Saintome, C. (2006) Human replication protein A unfolds telomeric G-quadruplexes. *Nucleic Acids Res.* **34**, 4857-4865

27. Safa, L., Delagoutte, E., Petruseva, I., Alberti, P., Lavrik, O., Riou, J.F., Saintomé, C. (2014) Binding polarity of RPA to telomeric sequences and influence of G-quadruplex stability. *Biochimie* **103**, 80–88

28. Boncina, M., Lah, J., Prislan, I., Vesnaver, G. (2012) Energetic basis of human telomeric DNA folding into G-quadruplex structures. *J. Am. Chem. Soc.* **134**, 9657-9663

29. Li, W., Hou, X.M., Wang, P.Y., Xi, X.G., Li, M. (2013) Direct measurement of sequential folding pathway and energy landscape of human telomeric G-quadruplex structures. *J. Am. Chem. Soc.* **135**, 6423-6426

30. Gray, R.D., Trent, J.O., Chaires, J.B. (2014) Folding and unfolding pathways of the human telomeric G-quadruplex. *J. Mol. Biol.* **426**, 1629-1650

31. Qureshi, M.H., Ray, S., Sewell, A.L., Basu, S. and Balci, H. (2012) Replication Protein A Unfolds G-Quadruplex Structures with Varying Degrees of Efficiency. *J Phys Chem B*. **116**, 5588-5594

32. Ray, S., Qureshi, M. H., Malcolm, D. W., Budhathoki, J. B., Celik, U. and Balci, H. (2013) RPA-Mediated Unfolding of Systematically Varying G-Quadruplex Structures. *Biophysical Journal* **104**, 2235–2245

33. Valton, A.L., Hassan-Zadeh, V., Lema, I., Boggetto, N., Alberti, P., Saintomé, C., Riou, J.F., Prioleau, M.N. (2014) G4 motifs affect origin positioning and efficiency in two vertebrate replicators. *EMBO J.* **33**, 732-746

34. Audry, J., Maestroni, L., Delagoutte, E., Gauthier, T., Nakamura, T.M., Gachet, Y., Saintomé, C., Géli, V., Coulon, S. (2015) RPA prevents G-rich structure formation at lagging strand telomeres to allow maintenance of chromosome ends. *EMBO J.* **34**, 1942-1958

35. Iftode, C., Borowiec, J.A. (2000) 5' / 3' molecular polarity of human replication protein A (hRPA) binding to pseudo-origin DNA substrates, *Biochemistry* **39**, 11970-11981

36. Favre, A. (1990) 4-thiouridine as an intrinsic photoaffinity probe of nucleic acid structure and interactions. *In Morrison,H. (ed.), Bioorganic Photochemistry*, Willey & Sons, New York, **1**, 379–425

37. Favre, A., Saintome, C., Fourrey, J.L., Clivio, P., Laugaa, P. (1998) Thionucleobases as intrinsic photoaffinity probes of nucleic acid structure and nucleic acid protein interactions. *J. Photochem. Photobiol. B* **42**, 109-124

38. Lavrik, O.I., Kolpashchikov, D.M., Nasheuer, H.P., Weisshart, K., Favre, A. (1998) Alternative conformations of human replication protein A are detected by crosslinks with

12

primers carrying a photoreactive group at the 30-end. *Febs Lett.* **441**, 186-190

39. Monchaud, D. and Teulade-Fichou, M.P. (2008) A hitchhiker's guide to G-quadruplex ligands. *Org. Biomol. Chem*. **6**, 627-636

40. Gomez, D., Paterski, R., Lemarteleur, T., Shin-Ya, K., Mergny, J.L. and Riou, J.F. (2004) Interaction of telomestatin with the telomeric single-strand overhang. *J. Biol. Chem*. **279**, 41487-41494

41. Pennarun, G., Granotier, C., Gauthier, L.R., Gomez, D., Hoffschir, F., Mandine, E., Riou, J.F., Mergny, J.L., Mailliet, P. and Boussin, F.D. (2005) Apoptosis related to telomere instability and cell cycle alterations in human glioma cells treated by new highly selective G-quadruplex ligands. *Oncogene* **24**, 2917-2928

42. Sidibe, A., Hamon, F., Largy, E., Gomez, D., Teulade-Fichou, M.P., Trentesaux, C. and Riou, J.F. (2012) Effects of a halogenated G-quadruplex ligand from the pyridine dicarboxamide series on the terminal sequence of XpYp telomere in HT1080 cells. *Biochimie* **94**, 2559-2568

43. Delagoutte, E., Heneman-Masurel, A. and Baldacci, G. (2011) Single-stranded DNA binding proteins unwind the newly synthesized double-stranded DNA of model miniforks. *Biochemistry* **50**, 932-944

44. de Laat, W.L,. Appeldoorn, E., Sugasawa, K., Weterings, E., Jaspers, N.G., Hoeijmakers, J.H. (1998) DNA-binding polarity of human replication protein A positions nucleases in nucleotide excision repair. *Genes Dev.* **12**, 2598-2609

45. Le, D.D., Di Antonio, M., Chana, L.K.M. and Balasubramanian, S. (2015) G-quadruplex ligands exhibit differential G-tetrad selectivity, *Chem. Commun.* **51**, 8048-8050

46. Mendoza, O., Gueddouda, M. M., Boule, J.B., Bourdoncle, A., Mergny, J.L. (2015) A fluorescence-based helicase assays: application to the screening of G-quadruplex ligands. *Nucleic Acids Res*. **43**, e71

47. Nguyen, B., Sokoloski, J., Galletto, R., Elson, E.L., Wold, M.S., Lohman, T.M. (2014) Diffusion of human replication protein A along single-stranded DNA. *J. Mol. Biol.* **426**, 3246-3261

48. Treuner, K., Ramsperger, Knippers, R. (1996) Replication protein A induces the unwinding of long double-stranded DNA regions. *J. Mol. Biol.* **259**, 104-112

49. Lao, Y., Lee, C.G., Wold, M.S. (1999) Replication protein A interactions with DNA. 2. Characterization of double-stranded DNA-binding/helix-destabilization activities and the role of the Zinc-finger domain in DNA interactions. *Biochemistry* **38**, 3974-3984

50. Byrd, A., Raney, K.D. (2015) A parallel quadruplex DNA is bound tightly but unfolded slowly by Pif1 helicase. *J. Biol. Chem.* **290**, 6482-6494

51. Boulé, J.B. and Zakian, V.A. (2006) Roles of Pif1-like helicases in the maintenance of genomic stability. *Nucleic Acids Res.* **34**, 4147-4153

52. Paeschke K., Bochman M.L., Garcia P.D., Cejka P., Friedman K.L., Kowalczykowski S.C., Zakian, V.A. (2013) Pif1 family helicases suppress genome instability at G-quadruplex motifs *Nature* **497**, 458-462

53. Bachrati, C.Z., Hickson, I.D. (2008) RecQ helicases: guardian angels of the DNA replication fork. *Chromosoma* **117**, 219-233

54. Hwang, H., Buncher, N., Opresko, P.L., Myong, S. (2012) POT1-TPP1 regulates telomeric overhang structural dynamics. *Structure* **20**, 1872-1880

55. Wu, C.G., Spies, M. (2013) Overview: What Are Helicases? *In Springer (ed.), Adv. in Exp. Med. Biol.,* New York Heidelberg Dordrecht London, **767**, 1-16

56. Delagoutte, E., von Hippel P.H. (2003) Helicase mechanisms and the coupling of helicases within macromolecular machines. Part I: Structures and properties of isolated helicases. *Q. Rev. Biophys*. **35**, 431-478

13

57. Delagoutte, E., von Hippel P.H. (2003) Helicase mechanisms and the coupling of helicases within macromolecular machines. Part II: Integration of helicases into cellular processes. *Q. Rev. Biophys.* **36**, 1-69

58. Gomes, X.V., Henricksen, L.A., Wold, M.S. (1996) Proteolytic mapping of human replication protein A: evidence for multiple structural domain and a conformational change upon interaction with single-stranded DNA. *Biochemistry*, **35**, 5586-5595

Footnotes

The abbreviations used are: hRPA, human Replication Protein A; G4, G-quadruplexes; DBD, DNA Binding Domain; EMSA, Electrophoretic mobility shift assays (EMSA); FRET, fluorescence resonance energy transfer, FAM, 6-carboxyfluoresceine; TAMRA, Tetramethylrhodamine

14

Figure legends

FIGURE 1. EMSA and FRET of htelo and extended htelo with hRPA. (A) EMSA of ^{32}P-htelo and ^{32}P-extended-htelo. Oligonucleotides (2 nM) were incubated with hRPA (from 5 to 100 nM) for 20 min at 20 °C; free DNA and hRPA-DNA complexes are indicated. 5t-htelo figure is composed of two gels separated by a line. (B, C) Quantification of EMSA: percentage of DNA in hRPA-DNA complexes as a function of hRPA concentration for htelo and oligonucleotides with 5-nt tails (B) and for htelo and oligonucleotides with 10-nt tails (C). (D) FRET efficiency (P) as a function of hRPA/FhteloT-10t (circles) and hRPA/10t-FhteloT (triangles) ratio (r); the oligonucleotide concentration was 100 nM and the protein concentration was from 100 to 1000 nM; error bars were < 10%.

FIGURE 2. Crosslinking experiments of htelo and extended htelo with hRPA. ^{32}P-labeled extended thiolated (S) htelo oligonucleotides (2 nM) were mixed with hRPA then irradiated at 10 °C for 30 min. SDS-PAGE (15%) was used to separate DNA crosslinked to RPA1 or RPA2 from free DNA. The relative percentage of DNA cross-linked with RPA1 and RPA2 subunits were quantified for each photoactivable DNA. Positions of photoactivable thiolated nucleotide are shown schematically above the gel image (lane 1: 10t-htelo-S0; lane 2: 10t-htelo-S10; lane 3: 10t-htelo-S20; lane 4: 10t-htelo-S31; lane 5: htelo-10t-S0; lane 6: htelo-10t-S10; lane 7: htelo-10t-S22; lane 8: htelo-10t-S31; lane M: molecular weight markers; lane 9: 10t-htelo-S0 without hRPA).

FIGURE 3. EMSA and FRET of htelo and extended htelo with hRPA, in the presence of G4 ligands. (A, B) Quantification of EMSA: percentage of DNA in hRPA-DNA complexes as a function of hRPA concentration for htelo with 5-nt tails (A) and htelo with 10-nt tails (B) in the presence and absence of telomestatin. ^{32}P-extended htelo (2 nM) was incubated with hRPA (from 5 to 100 nM) in the presence of 0.5 μM telomestatin and separated on a native 1% agarose gel. (C) Quantification of EMSA in the presence of different ligands: the percentage of inhibition of hRPA binding to htelo and extended htelo was calculated as (1-R)x100, where R is the ratio between the percentage of hRPA-DNA complexes in the presence and in the absence of ligands at 100 nM of hRPA. (D) FRET efficiency (P) as a function of hRPA/FhteloT-10t (circles) and hRPA/10t-FhteloT (triangles) ratio (r) in the presence of 360A (0.5 μM); the oligonucleotide concentration was 100 nM and the protein concentration was from 100 to 1000 nM; error bars were < 10%.

FIGURE 4. Fluorescence kinetic assays. Fluorescence emission of FAM was monitored as a function of time for a mixture of 10 nM of DNA construct (11s-htelo-dx (A), dx-htelo-11ss (B), 11ss-mut-dx (C), and dx-mut-11ss (D)) and 100 nM of Trap1, in the presence of different amounts of hRPA (5, 10, 15 or 20 equivalents). Once the steady-state was attained 100 nM of Trap2 was added to reaction wells in order to completely open the DNA construct and emission monitored until reaching again the steady-state of fluorescence emission. Two curves for each hRPA concentration are shown.

FIGURE 5. Model of G4 unfolding by RPA. (A) According to literature, hRPA binds to ssDNA in a sequential pathway with a defined spatial polarity: first it binds ssDNA in th 8-10 nt binding mode involving DBD-A and DBD-B of RPA1, then it lays-out toward 3' in the 30 nt binding mode involving DBD-C of RPA1 and DBD-D of RPA2. (B) When RPA binds to a single-stranded tail next to the 5' side of a G4, its sequential and spatial-oriented laying-out

15

from 5' toward 3' destabilizes and unfolds the G4 "in front" of it. (C) Conversely, when RPA binds to a single-stranded tail next to the 3' side of a G4, it laying-out toward 3' does not affect the G4 "behind" it. (D) Putative role of 5' to 3' unfolding directionality of RPA during telomere replication. RPA is recruited at telomeres with the replication machinery. ssDNA generated on the telomeric lagging strand template (G-rich) may fold into G4s. RPA contributes to the progression of the replication fork (which proceeds from 5' to 3' relative to the lagging strand template) by unfolding G4s from 5' to 3'.

16

Table 1: Sequences of oligonucleotides and *Tm* values

Name	Sequence	*Tm* °C K^{+}
htelo	GGGTTAGGGTTAGGGTTAGGG	68[a]
5t-htelo	tttttGGGTTAGGGTTAGGGTTAGGG	59.5[a]
htelo-5t	GGGTTAGGGTTAGGGTTAGGGttttt	61.5[a]
10t-htelo	ttttttttttGGGTTAGGGTTAGGGTTAGGG	59[a]
htelo-10t	GGGTTAGGGTTAGGGTTAGGGtttttttttt	60.5[a]
10t-FhteloT	tttttttttt-FAM-htelo-TAMRA	58[b] / 65[c]
FhteloT-10t	FAM-htelo-TAMRA-tttttttttt	60[b] / 65[c]
10t-htelo-S0	s4TttttttttttGGGTTAGGGTTAGGGTTAGGG	nd
10t-htelo-S10	tttttttttts4TGGGTTAGGGTTAGGGTTAGGG	nd
10t-htelo-S20	ttttttttttGGGTTAGGGs4TTAGGGTTAGGG	nd
10t-htelo-S31	ttttttttttGGGTTAGGGTTAGGGTTAGGGs4TT	nd
htelo-10t-S0	s4TGGGTTAGGGTTAGGGTTAGGGtttttttttt	nd
htelo-10t-S10	GGGTTAGGGs4TTAGGGTTAGGGtttttttttt	nd
htelo-10t-S22	GGGTTAGGGTTAGGGTTAGGGs4Ttttttttttt	nd
htelo-10t-S31	GGGTTAGGGTTAGGGTTAGGGttttttttts4TT	nd

nd: not determined, a) determined by absorbance at 295 nm as a function of temperature in the presence of 100 mM KCl, b, c) determined by fluorescein emission as a function of temperature in the presence of 10 mM KCl and 90 mM LiCl (b) or 100 mM KCl (c) (excitation wavelength 492 nm, emission wavelength 516 nm).

17

Table 2: Sequences of oligonucleotides for fluorescence kinetic assay

Name	Sequence
11ss-htelo-dx (construct 1): Dabcyl-labeled strand [1] FAM-labeled strand [1] Trap1 [1] Trap2 [1]	A_{11}GGGTTAGGGTTAGGGTTAGGGTATTCCGTTGAGCAGAG-Dabcyl FAM-CTCTGCTCAACGGAA TTCCGTTGAGCAGAG CTCTGCTCAACGGAATACCCTAACCCTAACCCTAACCCT$_{11}$
dx-htelo-11ss (construct 2): Dabcyl-labeled strand [2] FAM-labeled strand [2] Trap1 [2] Trap2 [2]	Dabcyl-GAGACGAGTTGCCTTATGGGTTAGGGTTAGGGTTAGGG-A_{11} AAGGCAACTCGTCTC-FAM GAGACGAGTTGCCTT T$_{11}$CCCTAACCCTAACCCTAACCCATAAGGCAACTCGTCTC
11ss-mut-dx (construct 3): Dabcyl-labeled strand [3] FAM-labeled strand [1] Trap1 [1] Trap 2 [3]	A_{11}TGGTGTGTAGTGTGGTTATTCCGTTGAGCAGAG-Dabcyl FAM-CTCTGCTCAACGGAA TTCCGTTGAGCAGAG CTCTGCTCAACGGAATAACCACACTACACACCAT$_{11}$
dx-mut-11ss (construct 4): Dabcyl-labeled strand [4] FAM-labeled strand [2] Trap1 [2] Trap2 [4]	Dabcyl-GAGACGAGTTGCCTTATTGGTGTGTAGTGTGGTA$_{11}$ AAGGCAACTCGTCTC-FAM GAGACGAGTTGCCTT T$_{11}$ACCACACTACACACCAATAAGGCAACTCGTCTC

18

A

htelo   5t-htelo   htelo-5t

10t-htelo   htelo-10t

hRPA-DNA complexes

Free DNA

B

C

D
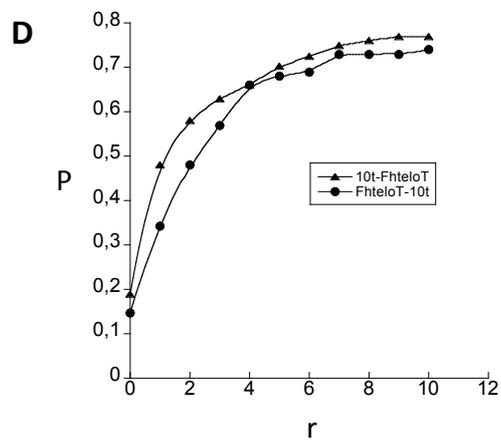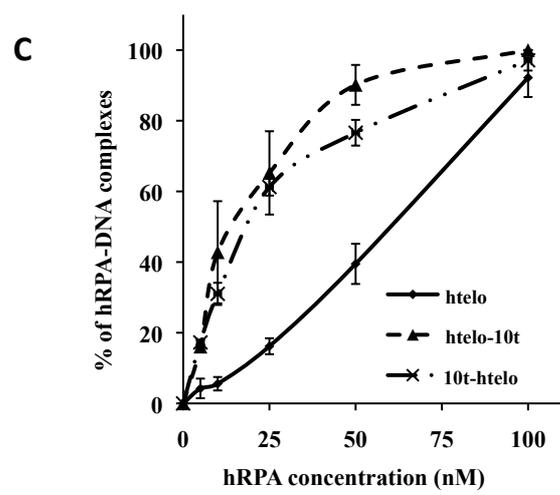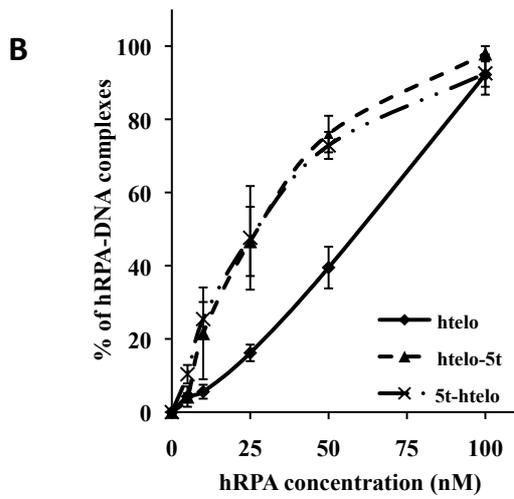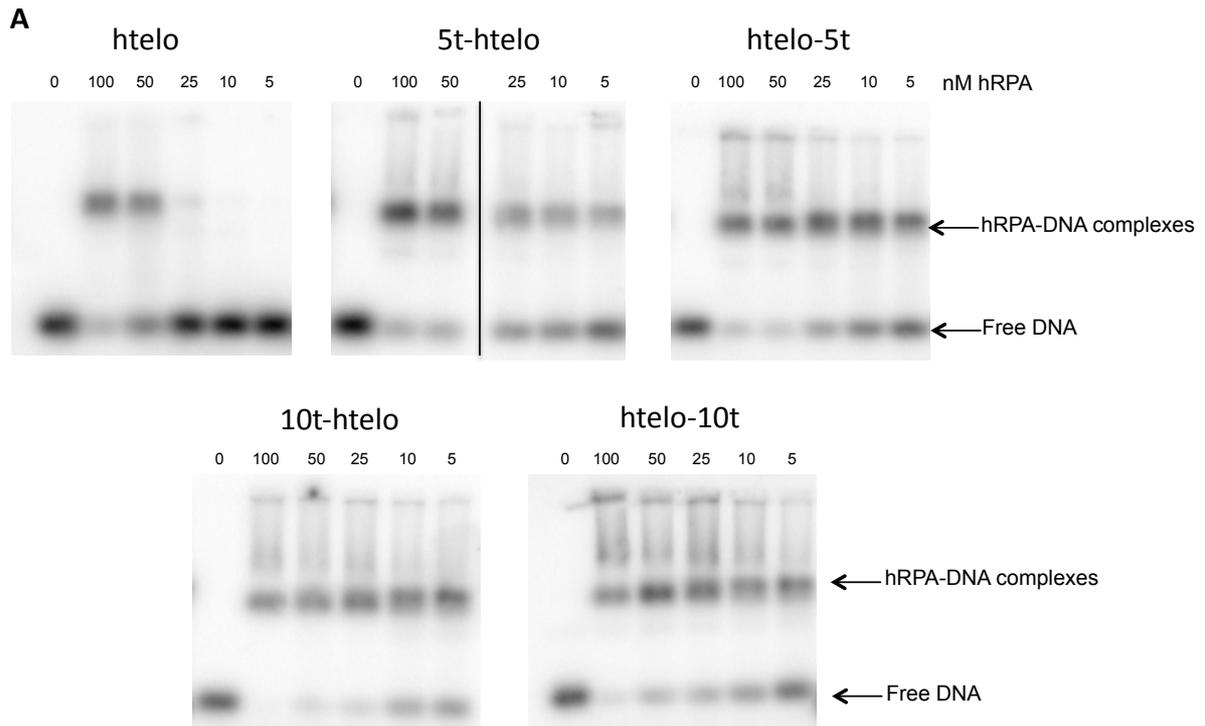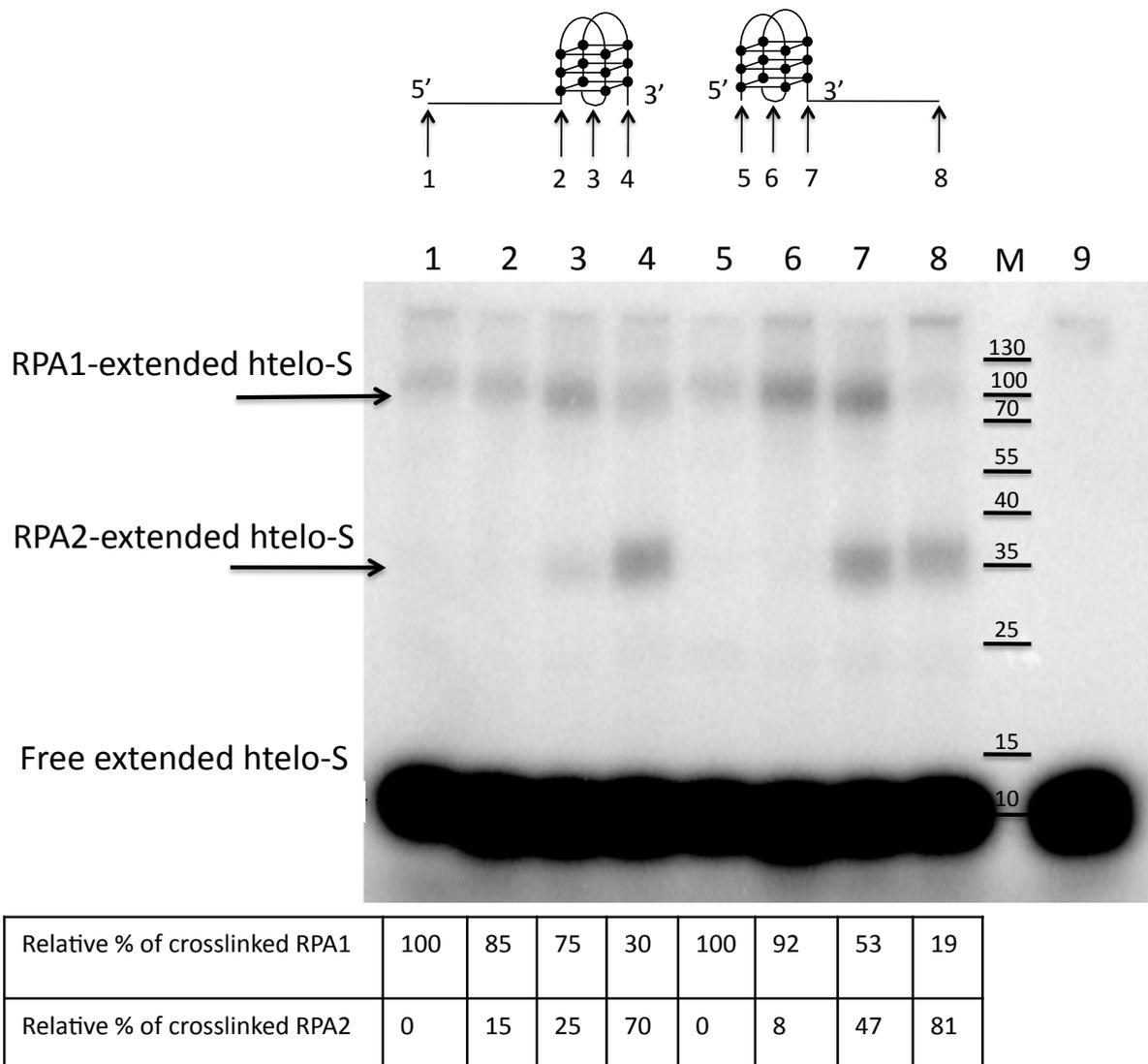
Figure 1

Figure 2

Figure 3

Figure 4

A

RPA1 RPA2 RPA3

8-10 nt binding mode   30 nt binding mode

B

C

D

5'

3'

5'

Lagging strand template

(GGGTTA)$_n$

3'

Replication fork

3'

5'

5'

3'
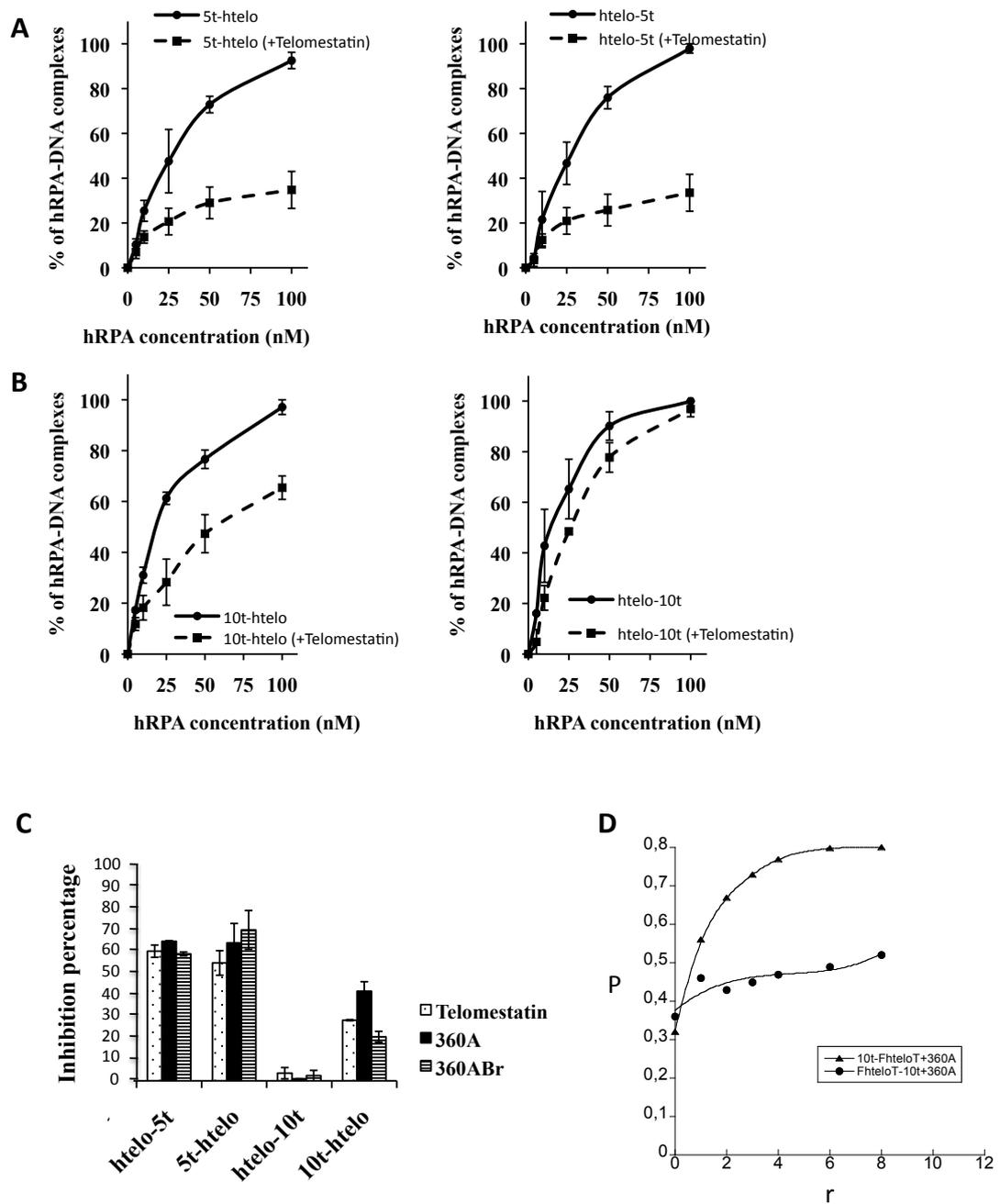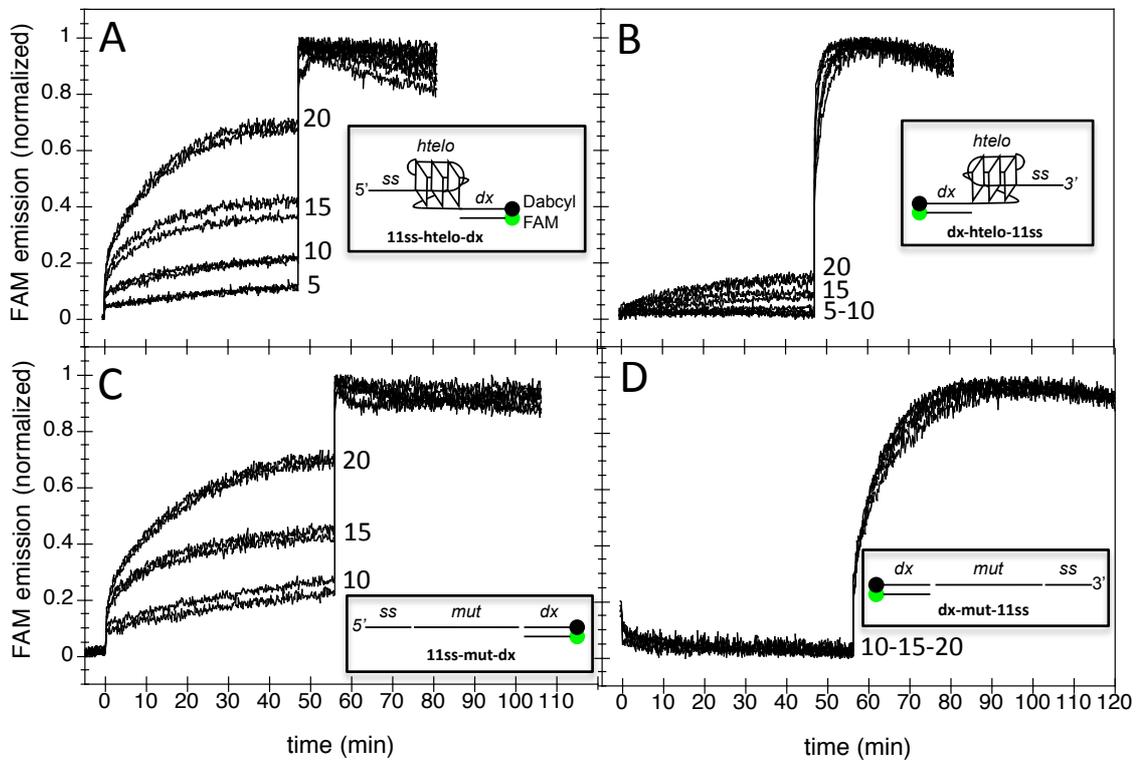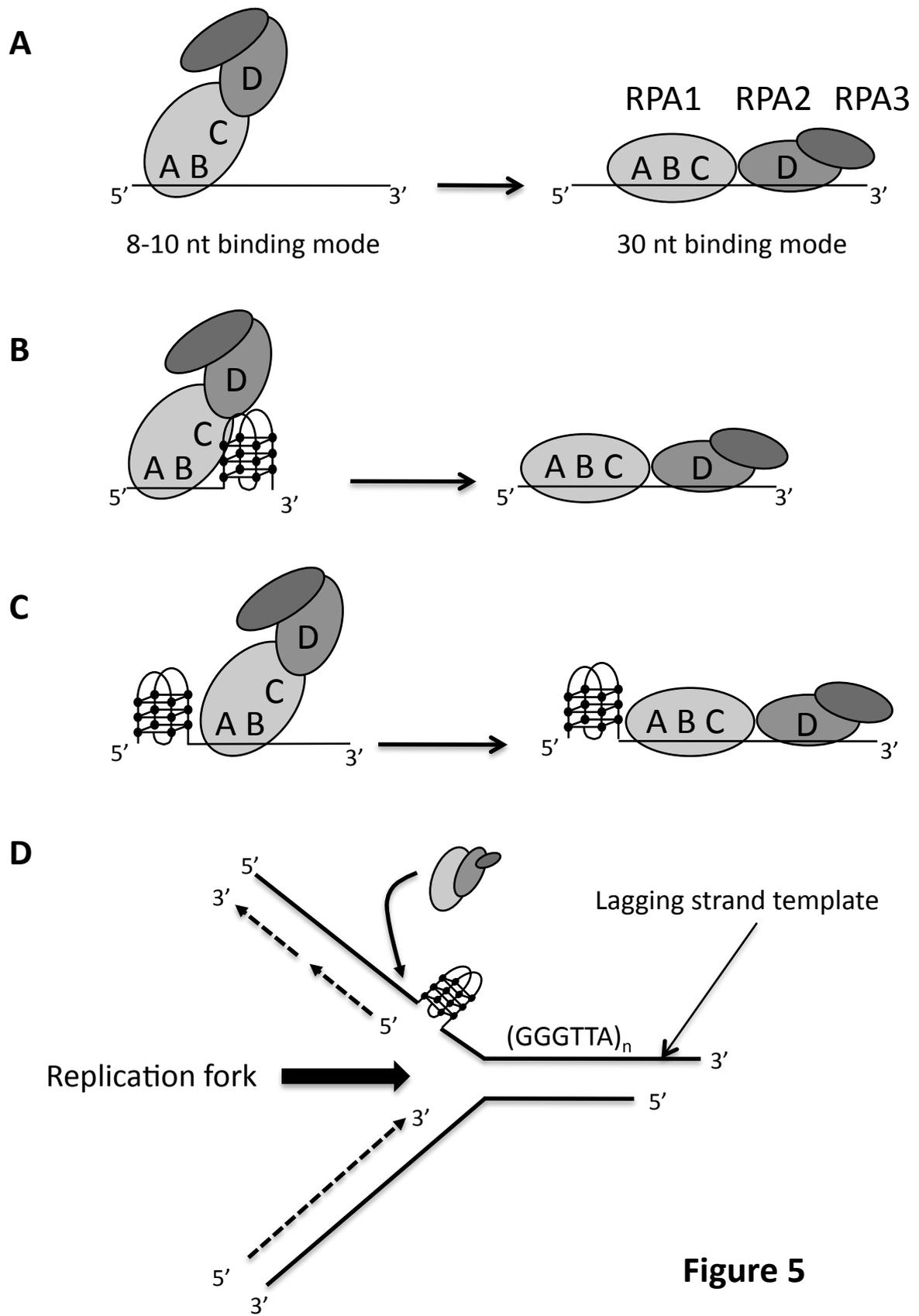
Figure 5

5' to 3' unfolding directionality of DNA secondary structures by replication protein A: G-quadruplexes and duplexes.

Layal Safa, Nassima Meriem Gueddouda, Frederic Thiebaut, Emmanuelle Delagoutte, Irina Petruseva, Olga Lavrik, Oscar Mendoza, Anne Bourdoncle, Patrizia Alberti, Jean-Francois Riou and Carole Saintome

J. Biol. Chem. published online July 19, 2016